

# CONSERVATIVE, SHOCK-CAPTURING TRANSPORT METHODS WITH NONCONSERVATIVE VELOCITY APPROXIMATIONS

CLINT DAWSON <sup>†</sup>

**Abstract.** Conservative high-resolution, or shock-capturing, methods have become widely used for modeling transport equations described by conservation laws. In many geoscience applications, the transport equation is coupled to a conservation or continuity equation for a velocity field. Depending on how the velocity is approximated, the continuity equation may or may not be satisfied, either locally or globally. In this paper, we discuss the effect this has on a typical high resolution scheme, and propose a correction which accounts for the fact that the velocity may be nonconservative. We present several numerical examples, and prove stability bounds and an *a priori* error estimate for the corrected method.

**Key words.** transport equations, conservation laws, conservative method, high resolution method, discontinuous Galerkin, nonconservative velocity fields

**AMS subject classifications.** 35Q35, 35L65 65N30, 65N15

**1. Introduction.** Consider the transport equation:

$$(1) \quad c_t + \nabla \cdot (uc) = 0, \quad (x, t) \in \Omega \times (0, T],$$

where  $\Omega$  is a bounded domain in  $\mathbb{R}^d$ ,  $d = 1, 2$ , or  $3$ , with Lipschitz boundary  $\partial\Omega$ , and  $T > 0$ . The quantity  $c$  might represent, for example, the concentration of some chemical component, which is transported through the region  $\Omega$  by the velocity  $u$ . The velocity  $u$  often satisfies a related conservation or continuity equation. For example, in flow through porous media, summing the transport equations over all components in the fluid, assuming the fluid is incompressible and no external sources and sinks are present, we obtain the continuity equation

$$(2) \quad \nabla \cdot u = 0.$$

The same continuity equation also arises in contaminant transport in surface water. Therefore, as a model problem, we will consider the transport equation (1), where the velocity satisfies (2). A more general transport equation might include diffusion and chemical reactions. In this paper, however, we are mostly interested in the approximation of the velocity  $u$ , which enters the equation predominantly through the advection term  $\nabla \cdot (uc)$ .

We supplement (1) with an initial condition

$$(3) \quad c(x, 0) = c^0(x), \quad \text{on } \Omega.$$

For boundary conditions, let  $n$  denote the unit outward normal to  $\Gamma \equiv \partial\Omega$ . We write  $\Gamma = \bar{\Gamma}_I \cup \bar{\Gamma}_O$ , where

$$(4) \quad \Gamma_I = \{x \in \partial\Omega : u \cdot n < 0\},$$

and

$$(5) \quad \Gamma_O = \{x \in \partial\Omega : u \cdot n \geq 0\}.$$

---

<sup>†</sup>Center for Subsurface Modeling - C0200; Texas Institute for Computational and Applied Mathematics; The University of Texas at Austin; Austin, TX 78712. This research was supported in National Science Foundation grants DMS-9873326 and DMS-9805491

On the inflow boundary we assume

$$(6) \quad c = c_I,$$

where  $c_I$  is specified.

Depending on the initial and boundary data, the solution  $c$  may have sharp fronts or even discontinuities. In recent years, various types of conservative high resolution or shock capturing methods have been proposed for solving such equations, see [16] for a survey of such methods in one space dimension. A number of authors have adopted this type of approach for geoscience applications, see for example [1, 4, 12, 13, 15, 14, 19, 20, 22]. In this paper, we will consider a variant of this approach based on the discontinuous Galerkin method, as developed by Cockburn, Shu *et al* in a number of papers [6, 9, 8, 10, 7].

Given a partition of the domain  $\Omega$  into elements  $\Omega_e$ , we multiply (1) by a test function  $w$  and integrate over  $\Omega_e$ :

$$(7) \quad \int_{\Omega_e} c_t w \, dx - \int_{\Omega_e} c u \cdot \nabla w \, dx + \int_{\partial\Omega_e} u \cdot n_e c w \, dx = 0,$$

where  $n_e$  is the unit outward normal to  $\partial\Omega_e$ . Taking  $w = 1$  on  $\Omega_e$ , (7) is simply a statement that the accumulation of  $c$  in  $\Omega_e$  is due to what flows in and out of the boundary, that is, the quantity  $c$  is conserved over  $\Omega_e$ . The basic idea of the discontinuous Galerkin method is to approximate  $c$  on  $\Omega_e$  by a polynomial function  $C$ , and takes  $w$  to lie in the same space as  $C$ . On  $\partial\Omega_e$ ,  $c$  is approximated by upwinding. This type of numerical approach can be shown to be  $L^2$  stable and one can also prove *a priori* error estimates, see for example [11]. In certain simpler cases one can prove the scheme satisfies a maximum principle. Numerically, one finds that the scheme accurately resolves sharp fronts and is stable, provided the higher order polynomial terms in  $C$  are controlled to prevent oscillations [10].

Suppose the velocity  $u$  is approximated by  $U$ . Depending on the type of numerical method used,  $U$  may not satisfy (2). The question then is how does this effect the method? Take, for example, a simple one space dimensional case. In one dimension, (2) implies that  $u$  is a constant. But suppose  $u \approx U = U(x)$ , which is not a constant, and assume  $u, U > 0$ . Take the domain  $\Omega = [0, 1]$ , and partition it into elements  $B_j = [x_{j-1/2}, x_{j+1/2}]$  of length  $h$ . Approximate  $c$  by a constant  $C_j$  on  $B_j$ . Using a forward Euler time discretization with time step  $\Delta t$ , we obtain the upwind scheme

$$(8) \quad \frac{C_j^{k+1} - C_j^k}{\Delta t} + \frac{U_{j+1/2} C_j^k - U_{j-1/2} C_{j-1}^k}{h} = 0,$$

where  $\Delta t$  is the time step,  $k$  represents the time level  $t^k = k\Delta t$ , and  $U_{j+1/2} = U(x_{j+1/2})$ . Now suppose, for example, that  $C_j^k = C_{j-1}^k = 1$ , then if  $U = u$  we would have  $C_j^{k+1} = 1$ . However, by (8),

$$(9) \quad C_j^{k+1} = 1 - \frac{\Delta t}{h} [U_{j+1/2} - U_{j-1/2}],$$

which may be quite different from one, depending on how close  $U$  is to satisfying (2). More specifically, suppose the true velocity  $u = 1$  and  $U(x) = 1 + .05 \cos(20\pi x)$ . Then  $U$  approximates  $u$  with 5 % error, but the error in  $U_x$  is much larger, in particular  $-\pi \leq U_x \leq \pi$ . Taking  $c^0 = 0$ ,  $c_I = 1$ ,  $h = 1/100$  and  $\Delta t = .5 * h$ , we get the

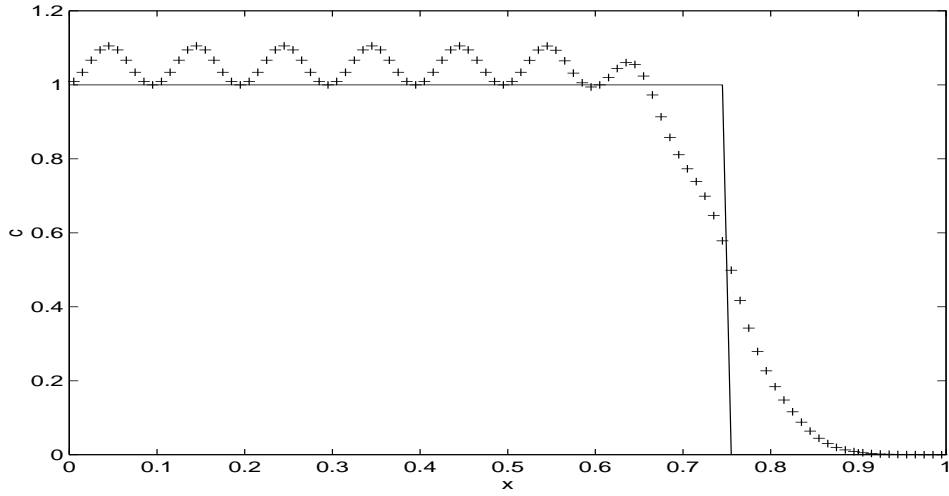


FIG. 1. Approximate (+) vs. analytic solution at  $t=.75$  with velocity  $U$ .

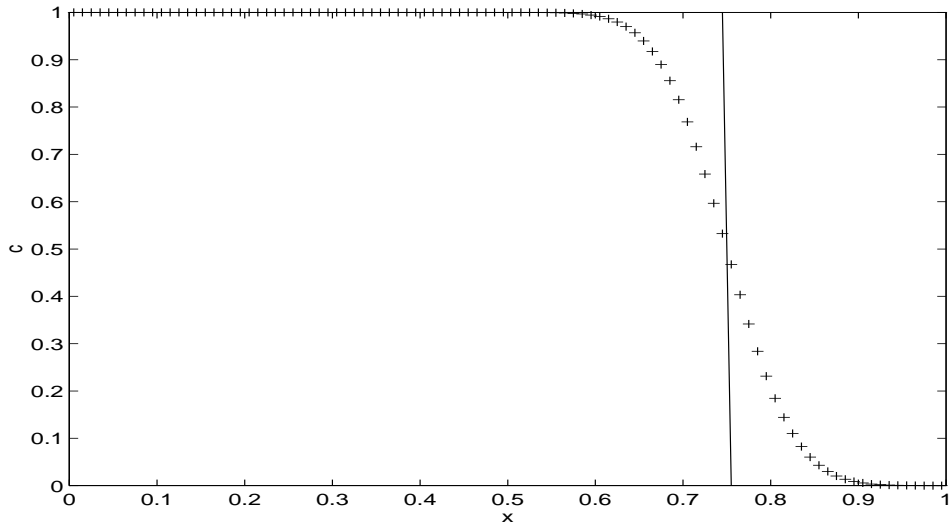


FIG. 2. Approximate (+) vs. analytic solution at  $t=.75$  with velocity  $u$ .

numerical solution shown in Figure 1 for the method (8). This solution is oscillatory and obviously violates the maximum principle which the true solution satisfies. When replacing  $U$  in (8) by the true  $u$ , we get the solution in Figure 2, which is numerically diffusive but not oscillatory.

Consider a two-dimensional example. Suppose the domain  $\Omega$  is the unit square and we discretize  $\Omega$  into grid blocks  $B_{ij} = [x_{i-1/2}, x_{i+1/2}] \times [y_{j-1/2}, y_{j+1/2}]$  of size  $h * h$ . Furthermore, suppose  $c \approx C$ , where  $C$  is a constant  $C_{ij}$  on  $B_{ij}$ . Then, the

extension of (7) and (8) is

$$(10) \quad \frac{C_{ij}^{k+1} - C_{ij}^k}{\Delta t} + \int_{\partial B_{ij}} (C^k)^u U \cdot n_{ij} ds = 0.$$

Now suppose  $C^k = 1$  in a sufficiently large neighborhood of  $B_{ij}$ , so that  $(C^k)^u = 1$ , then

$$(11) \quad \begin{aligned} C_{ij}^{k+1} &= 1 - \Delta t \int_{\partial B_{ij}} U \cdot n_{ij} ds \\ &= 1 - \Delta t \int_{B_{ij}} \nabla \cdot U dx, \end{aligned}$$

which again may not be equal to one, depending on  $U$ .

From these examples it would seem highly desirable that however one approximates the velocity  $u$ , the approximation should also satisfy (2), at least in the integral sense over each element. But satisfying (2) is not always built-in to the numerical method used to calculate  $u$ . For example, when applying a standard Galerkin method to the flow equation in porous media, the computed velocity will most likely not satisfy (2). Another example comes from surface water hydrodynamics. Many standard hydrodynamic simulators, for example ADCIRC [17] or RMA10 [2], do not produce a velocity which satisfies the continuity equation (2). However, when using these velocities in a conservative, shock-capturing water quality transport code, such as CE-QUAL-ICM [13], it is usually expected that the continuity condition has been satisfied. This problem has motivated recent work on projection methods, whereby a velocity field is postprocessed so that conservation is enforced [5]. Such postprocessing involves solving an elliptic equation at each timestep the velocity is needed, therefore it is a time-consuming computation.

In this paper, we present a simple correction procedure to the discontinuous Galerkin method outlined above which accounts for a possibly nonconservative velocity field. This same correction procedure could be used in any shock-capturing method. This approach is very easy to implement, and does not involve any modifications to the approximate velocity field itself. We will prove some stability and error bounds for the method. Our error analysis is valid for any approximation  $U$  to the velocity  $u$ .

The paper is outlined as follows. In the next section, we define the correction procedure and give some numerical examples. In Section 3, we comment on the stability of the approach and derive an *a priori* error estimate. Finally, in Section 4, a two-dimensional example from flow and transport in porous media is presented.

**2. Method formulation.** We first define some notation. Let  $(\cdot, \cdot)_D$  denote the  $L^2(D)$  inner product, where we omit  $D$  if  $D = \Omega$ . To distinguish integration over domains  $D \in \mathbb{R}^{d-1}$  (e.g., surfaces or lines), we will use the notation  $\langle \cdot, \cdot \rangle_D$ . Let  $\|\cdot\|_{p,D}$  denote the  $L^p(D)$  norm, where again we omit  $D$  if  $D = \Omega$  and we omit  $p$  if  $p = 2$ . Norms in other Sobolev spaces  $W(D)$  are denoted by  $\|\cdot\|_{W(D)}$ .

The ‘‘corrected’’ method for a nonconservative velocity field is motivated by the following simple observation. By (2), (1) can be written as

$$c_t + u \cdot \nabla c = 0.$$

If  $U \approx u$ , then

$$(12) \quad 0 \approx c_t + U \cdot \nabla c = c_t + \nabla \cdot (Uc) - c \nabla \cdot U.$$

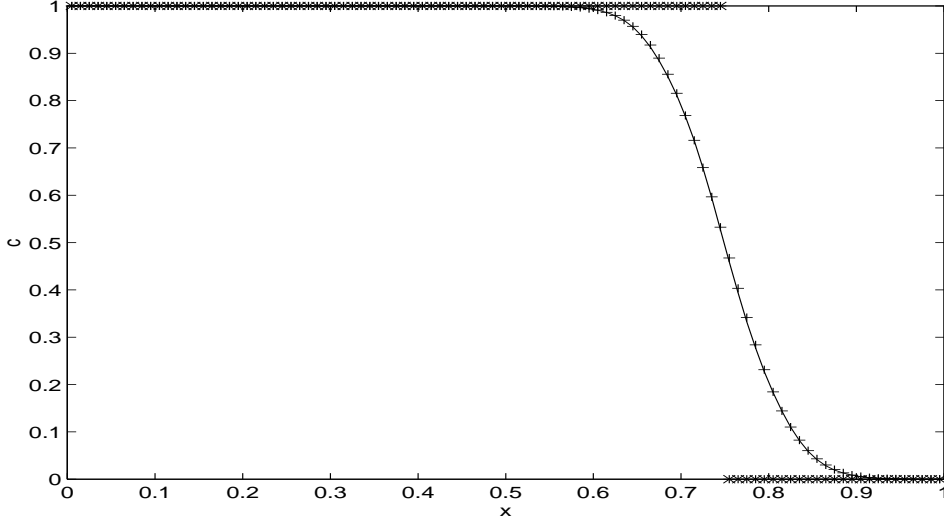


FIG. 3. *New method with velocity  $U$  (solid line), with true velocity  $u$  (+) and analytic solution (\*) at  $t=.75$ .*

Thus the “correction term” is  $-c\nabla \cdot U$ .

Let us revisit (8) with this correction term added. The method is now

$$(13) \quad \frac{C_j^{k+1} - C_j^k}{\Delta t} + \frac{U_{j+1/2} C_j^k - U_{j-1/2} C_{j-1}^k}{h} - C_j^{k+1} \frac{U_{j+1/2} - U_{j-1/2}}{h} = 0.$$

First, note that if  $C_j^k = C_{j-1}^k =$  any constant  $C^*$ , then  $C_j^{k+1} = C^*$ , as it should be. If we apply this new method to the problem whose results are given in Figures 1 and 2, we obtain the result in Figure 3. Here we have plotted the numerical solution given by (13) as well as the numerical solution obtained from (8) with the true velocity  $u = 1$ . Notice that there is virtually no difference between the two solutions.

We now describe a general corrected method for a discontinuous Galerkin approximation of (1) in semidiscrete form. Let  $\{\mathcal{T}_h\}_{h>0}$  denote a family of finite element partitions of  $\Omega$  such that no element  $\Omega_e$  crosses the boundaries of  $\Gamma_I$  or  $\Gamma_O$ , where  $h_e$  is the element diameter and  $h$  the maximal element diameter. We also assume that each element  $\Omega_e$  has a Lipschitz boundary  $\partial\Omega_e$ . Let  $n_e$  denote the unit outward normal vector to  $\partial\Omega_e$ , with  $n_e = n$  on  $\Gamma$ . Then, for  $x \in \partial\Omega_e$  we define

$$w^-(x) = \lim_{s \rightarrow 0^-} w(x + sn_e),$$

and

$$w^+(x) = \lim_{s \rightarrow 0^+} w(x + sn_e).$$

Let  $W_{h,e} \subset H^1(\Omega_e)$  denote the set of all polynomials of degree at most  $k_e$  defined on  $\Omega_e$ .

On  $\Omega_e$ , we approximate  $c(\cdot, t)$  by  $C(\cdot, t) \in W_{h,e}$ , where  $C$  satisfies

$$(14) \quad (C(\cdot, 0) - c^0, w)_{\Omega_e} = 0, \quad w \in W_{h,e},$$

and for  $t > 0$ ,

$$(15) \quad (C_t, w)_{\Omega_e} - (UC, \nabla w)_{\Omega_e} + \langle C^u U \cdot n_e, w^- \rangle_{\partial\Omega_e} - (C\nabla \cdot U, w)_{\Omega_e} = 0, \quad w \in W_{h,e}.$$

Here, the upwind value  $C^u$  is determined on  $\partial\Omega_e$  by

$$(16) \quad C^u = \begin{cases} C^-, & u \cdot n_e \geq 0, \\ C^+, & u \cdot n_e < 0, \end{cases}$$

with  $C^+ = c_I$  when  $\partial\Omega_e$  intersects  $\Gamma_I$ .

As we will see below, our new approach satisfies similar stability bounds to the numerical solution obtained with the analytic velocity  $u$ . The accuracy of the approach depends of course on how well  $U$  approximates  $u$  and how closely  $U$  satisfies (2).

As we noted above in the one dimensional case, if  $C(\cdot, t)$  is a constant in the elements around  $\Omega_e$ , then  $C(\cdot, t + \Delta t)$  should equal this same constant in  $\Omega_e$ , for  $\Delta t$  sufficiently small. For example, suppose at some time  $t$ ,  $C = 1$  in a sufficiently large neighborhood of  $\Omega_e$ , so that  $C^u = 1$  on  $\partial\Omega_e$  when evaluated explicitly. Taking  $w = 1$  in (15), we find that

$$(17) \quad (C_t, 1)_{\Omega_e} - (C\nabla \cdot U, 1)_{\Omega_e} + \langle U \cdot n_e, 1 \rangle_{\partial\Omega_e} = 0.$$

Integrating in time from  $t$  to  $t + \Delta t$  and evaluating the second term in (17) implicitly, we find,

$$(C(\cdot, t + \Delta t), 1)_{\Omega_e} - \Delta t (C(\cdot, t + \Delta t) \nabla \cdot U, 1)_{\Omega_e} + \Delta t (\nabla \cdot U, 1)_{\Omega_e} = (C(\cdot, t), 1)_{\Omega_e},$$

or

$$(C(\cdot, t + \Delta t)(1 - \Delta t \nabla \cdot U), 1)_{\Omega_e} = (1 - \Delta t \nabla \cdot U, 1)_{\Omega_e}.$$

Thus  $C = 1$  on  $\Omega_e$ .

One drawback of (15) is that it is no longer globally conservative. Setting  $w = 1$ , summing over all elements, and integrating in time we have

$$\begin{aligned} \sum_e \int_{\Omega_e} C(\cdot, t) dx &= \sum_e \int_{\Omega_e} c^0 dx \\ &\quad - \int_0^t \left[ \int_{\Gamma_I} c_I U \cdot n ds dt + \int_{\Gamma_O} C^- U \cdot n - \sum_e \int_{\Omega_e} C \nabla \cdot U dx \right] dt. \end{aligned}$$

The last term on the right hand side is the conservation error, and the magnitude of this term obviously depends on how close  $\nabla \cdot U$  is to zero.

Before concluding this section, we present a few more numerical examples based on the one dimensional case discussed above. First, assume the error in the velocity is increased by setting  $U = 1 + .1 \cos(20\pi x)$ . In Figure 4, we have plotted three numerical solutions: 1) the method presented above, 2) the method without the correction term, and 3) the method with the analytic velocity  $u = 1$ . Note that solutions 1 and 3 are again very close, while solution 2 is highly oscillatory. Next, we assume  $U = 1 + .1 \sin(20\pi x)$ . The same three solutions are plotted in Figure 5, and similar behavior is observed. In this case, since  $U(0) = u(0)$  and  $U(1) = u(1)$ , the solution without the correction preserves mass in the same way that the solution

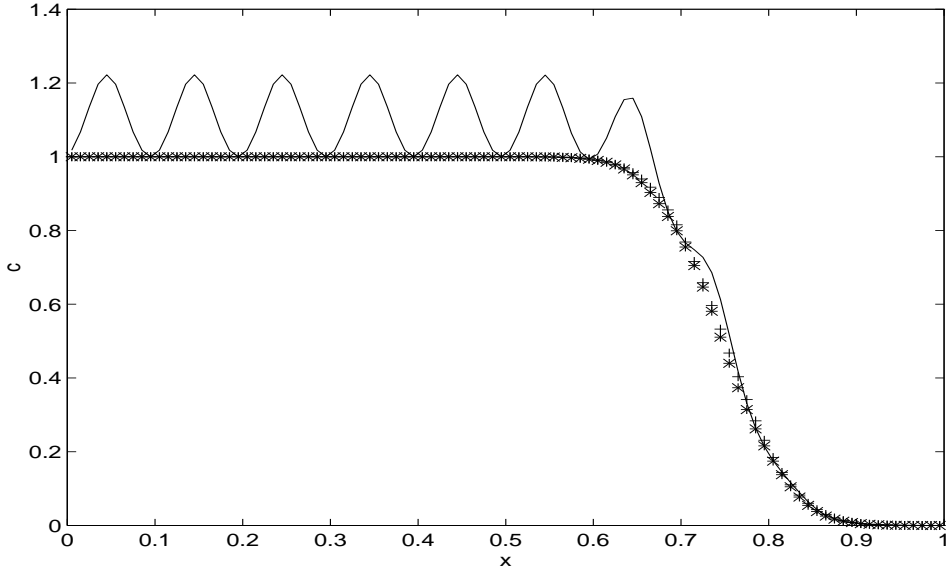


FIG. 4. *New method with velocity  $U = 1 + .1 \cos(20\pi x)$  (+), with true velocity  $u = 1$  (\*) and without correction (solid line) at  $t=.75$ .*

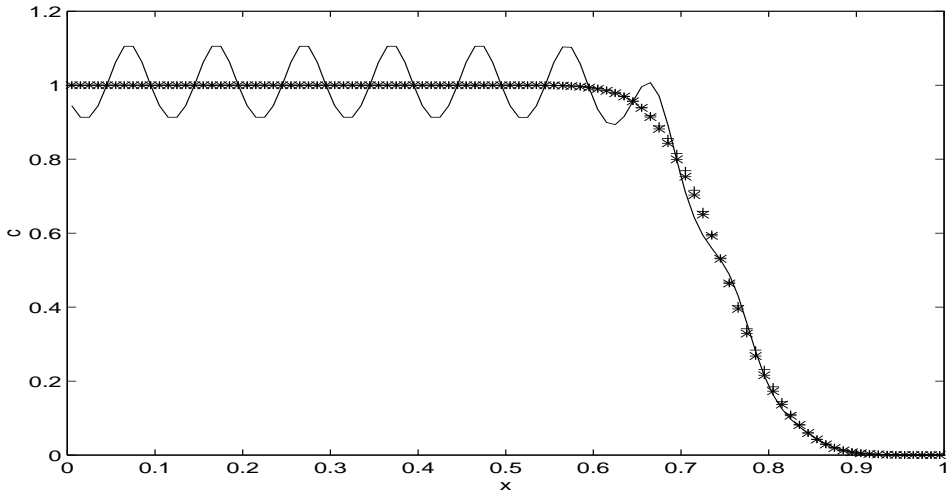


FIG. 5. *New method with velocity  $U = 1 + .1 \sin(20\pi x)$  (+), with true velocity  $u$  (\*) and without correction (solid line) at  $t=.75$ .*

with  $U = u$  does. In Figure 6, we show the same three cases with  $h = 1/1000$ . In this case, solutions 1) and 3) are much sharper, but solution 2) is still very oscillatory.

The accuracy of the corrected method does of course depend on the accuracy of the velocity approximation, as we will see in the analysis below. Suppose we dramatically increase the error in the velocity, by setting  $U = 1 + .5 \sin(20\pi x)$ . In Figure 7, we compare solutions 1 and 3 for  $h = 1/1000$ , and see that the solutions are very far apart.

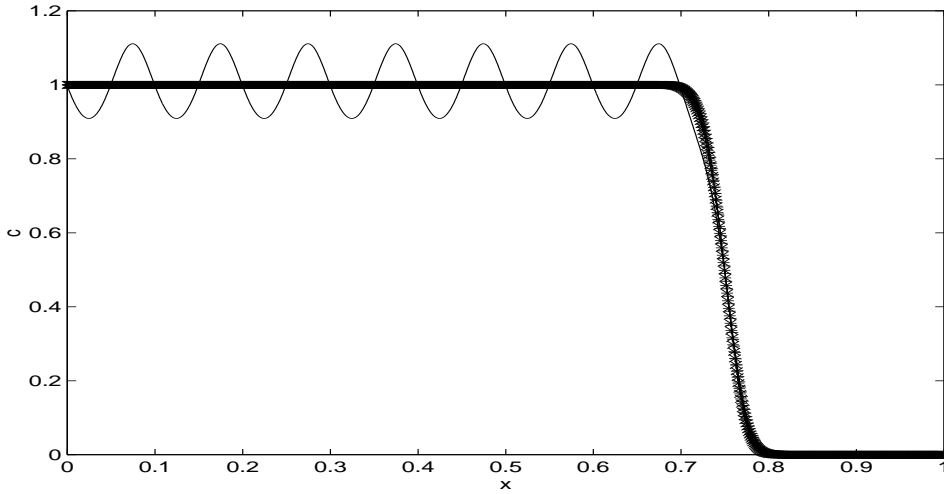


FIG. 6. New method with velocity  $U = 1 + .1 \sin(20\pi x)$  (+), with true velocity  $u$  (\*) and without correction (solid line) at  $t=.75$ ;  $h = 1/1000$ .

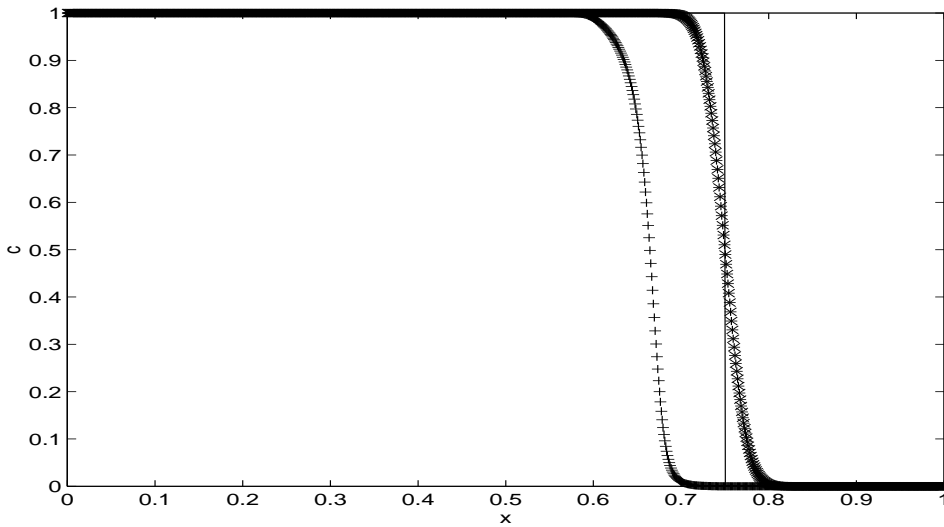


FIG. 7. New method with velocity  $U = 1 + .5 \sin(20\pi x)$  (+), with true velocity  $u$  (\*) and true solution (solid line) at  $t=.75$ ;  $h = 1/1000$ .

**3. Stability and error analysis.** In this section we present some stability bounds and *a priori* error estimates for the method (15) above.

Assume the CFL constraint

$$(18) \quad \frac{u\Delta t}{h} \leq 1.$$

Consider the one-dimensional case discussed in Section 1. If  $U = u > 0$ , and  $C_{\max}^k =$

$\max_j |C_j^k|$ , then by (13),

$$\begin{aligned}
(19) \quad |C_j^{k+1}| &= \left| C_j^k - \frac{u\Delta t}{h} [C_j^k - C_{j-1}^k] \right| \\
&= \left| \left(1 - \frac{u\Delta t}{h}\right) C_j^k + \frac{u\Delta t}{h} C_{j-1}^k \right| \\
&\leq \left(1 - \frac{u\Delta t}{h}\right) |C_j^k| + \frac{u\Delta t}{h} |C_{j-1}^k| \\
&\leq \left(1 - \frac{u\Delta t}{h} + \frac{u\Delta t}{h}\right) C_{\max}^k \\
&= C_{\max}^k,
\end{aligned}$$

where we have used (18) to note that  $1 - u\Delta t/h \geq 0$ . Thus  $\max_j |C_j^{k+1}| \leq C_{\max}^k$ .

Now assume  $u \approx U(x) > 0$ , and

$$(20) \quad 0 < \max_x \frac{\Delta t U(x)}{h} < 1.$$

Then rearranging terms in (13),

$$\begin{aligned}
(21) \quad &\left| 1 - \frac{\Delta t}{h} (U_{j+1/2} - U_{j-1/2}) \right| |C_j^{k+1}| \\
&= \left| \left[ 1 - \frac{\Delta t U_{j+1/2}}{h} \right] C_j^k + \frac{\Delta t U_{j-1/2}}{h} C_{j-1}^k \right| \\
&\leq \left[ 1 - \frac{\Delta t}{h} (U_{j+1/2} - U_{j-1/2}) \right] C_{\max}^k,
\end{aligned}$$

since, by (20),

$$(22) \quad 0 < 1 - \frac{\Delta t}{h} U_{j+1/2} < 1 - \frac{\Delta t}{h} (U_{j+1/2} - U_{j-1/2}).$$

Thus by (21),

$$(23) \quad |C_j^{k+1}| \leq C_{\max}^k,$$

and our corrected method also satisfies the  $L^\infty$  stability bound.

Next, we derive an *a priori* error estimate for the general method (15). We assume  $U$  is any approximation to the true velocity  $u$ , and  $U$  may or may not satisfy (2). We will compare  $C$  to  $\Pi c$ , where  $\Pi c$  is the  $L^2(\Omega_e)$  projection of  $c$  into  $W_{h,e}$ , which satisfies

$$(24) \quad (c - \Pi c, w)_{\Omega_e} = 0, \quad w \in W_{h,e}.$$

We also define  $\Pi c^u$  similar to  $C^u$ , see (16).

Define  $\psi = C - \Pi c$ , and  $\theta = c - \Pi c$ . Then, subtracting (7) from (15), and rearranging terms, we find

$$\begin{aligned}
(25) \quad &(\psi_t, w)_{\Omega_e} - (U\psi, \nabla w)_{\Omega_e} + \langle \psi^u U \cdot n_e, w^- \rangle_{\partial\Omega_e} \\
&= (\theta_t, w)_{\Omega_e} + ((U - u)\Pi c, \nabla w)_{\Omega_e} - (u\theta, \nabla w)_{\Omega_e} + \langle (c - \Pi c^u)U \cdot n_e, w^- \rangle_{\partial\Omega_e} \\
&\quad + \langle c(u - U) \cdot n_e, w^- \rangle_{\partial\Omega_e} + (\psi \nabla \cdot U, w)_{\Omega_e} + (\Pi c \nabla \cdot U, w)_{\Omega_e}.
\end{aligned}$$

Below we will sum (25) over all elements in the mesh. Let  $\gamma_l$  denote an interior edge in the mesh, and let  $n_l$  denote a unit vector normal to  $\gamma_l$ . For  $x \in \gamma_l$ , let

$$w^L = \lim_{s \rightarrow 0^-} w(x + sn_l),$$

and

$$w^R = \lim_{s \rightarrow 0^+} w(x + sn_l).$$

Define

$$[w] = w^R - w^L,$$

and

$$\bar{w} = \frac{1}{2}(w^R + w^L).$$

We also note that, consistent with the definition (16) above,

$$(26) \quad w^u = \begin{cases} w^L, & U \cdot n_l \geq 0, \\ w^R, & U \cdot n_l < 0. \end{cases}$$

Let  $w^d$  denote the ‘‘downwind’’ value on  $\gamma_l$ , then

$$(27) \quad [w] = \begin{cases} -(w^u - w^d), & U \cdot n_l \geq 0, \\ w^u - w^d, & U \cdot n_l < 0. \end{cases}$$

Suppose  $\partial\Omega_e$  intersects an interior edge  $\gamma_l$ . Then, if  $n_e = n_l$ ,

$$(28) \quad \langle w^u U \cdot n_e, w^- \rangle_{\partial\Omega_e \cap \gamma_l} = \langle w^u U \cdot n_l, w^L \rangle_{\partial\Omega_e \cap \gamma_l},$$

otherwise

$$(29) \quad \langle w^u U \cdot n_e, w^- \rangle_{\partial\Omega_e \cap \gamma_l} = -\langle w^u U \cdot n_l, w^R \rangle_{\partial\Omega_e \cap \gamma_l}.$$

Either way, summing over all elements whose boundaries intersect  $\gamma_l$ , we find

$$(30) \quad \sum_e \langle w^u U \cdot n_e, w^- \rangle_{\partial\Omega_e \cap \gamma_l} = -\langle w^u U \cdot n_l, [w] \rangle_{\gamma_l}.$$

In order to carry out the error estimate, we assume

**A1.** The velocity  $U$  satisfies the same conditions as  $u$  does on the inflow and outflow boundaries  $\Gamma_I$  and  $\Gamma_O$ .

**A2.** For  $h$  sufficiently small,

$$T \|\nabla \cdot U\|_\infty \leq \frac{1}{2},$$

where  $T > 0$  is the final time.

Summing (25) over all elements, and setting  $w = \psi$ , we find

$$(31) \quad \begin{aligned} & \sum_e [(\psi_t, \psi)_{\Omega_e} - (U\psi, \nabla\psi)_{\Omega_e}] - \sum_l \langle U \cdot n_l \psi^u, [\psi] \rangle_{\gamma_l} + \langle U \cdot n \psi^-, \psi^- \rangle_{\Gamma_O} \\ &= \sum_e [(\theta_t, \psi)_{\Omega_e} + ((U - u)\Pi c, \nabla\psi)_{\Omega_e} - (u\theta, \nabla\psi)_{\Omega_e} + (\nabla \cdot U, \psi^2)_{\Omega_e} \\ & \quad + (\Pi c \nabla \cdot U, \psi)_{\Omega_e}] \\ & \quad - \sum_l [\langle U \cdot n_l (c - \Pi c^u), [\psi] \rangle_{\gamma_l} - \langle (u - U) \cdot n_l c, [\psi] \rangle_{\gamma_l}] \\ & \quad + \langle U \cdot n (c - \Pi c^-), \psi^- \rangle_{\Gamma_O} + \langle (u - U) \cdot n c, \psi^- \rangle_{\Gamma_O}. \end{aligned}$$

Consider

$$(32) \quad - \sum_l \langle U \cdot n_l, \psi^u[\psi] \rangle_{\gamma_l} = -\frac{1}{2} \sum_l \langle U \cdot n_l, (\psi^u - \psi^d)[\psi] \rangle_{\gamma_l} - \sum_l \langle U \cdot n_l, \bar{\psi}[\psi] \rangle_{\gamma_l}.$$

By (16) and (27), the first term on the right of (32) becomes

$$\frac{1}{2} \sum_l \langle |U \cdot n_l|, [\psi]^2 \rangle_{\gamma_l}.$$

The second term becomes

$$\begin{aligned} -\frac{1}{2} \sum_l \langle U \cdot n_l, (\psi^R)^2 - (\psi^L)^2 \rangle_{\gamma_l} &= \frac{1}{2} \sum_e \int_{\Omega_e} \nabla \cdot (U \psi^2) dx - \frac{1}{2} \langle U \cdot n, (\psi^-)^2 \rangle_{\Gamma} \\ &= \frac{1}{2} \sum_e \int_{\Omega_e} (\nabla \cdot U) \psi^2 dx + \sum_e \int_{\Omega_e} \psi U \cdot \nabla \psi dx \\ &\quad + \frac{1}{2} \langle |U \cdot n|, (\psi^-)^2 \rangle_{\Gamma_I} - \frac{1}{2} \langle U \cdot n, (\psi^-)^2 \rangle_{\Gamma_O}. \end{aligned}$$

Thus, the second, third and fourth terms on the left side of (31) combine as follows,

$$\begin{aligned} (33) \quad & - \sum_e (U \psi, \nabla \psi)_{\Omega_e} - \sum_l \langle U \cdot n_l, \psi^u[\psi] \rangle_{\gamma_l} + \langle U \cdot n, (\psi^-)^2 \rangle_{\Gamma_O} \\ &= \frac{1}{2} \sum_l \langle |U \cdot n_l|, [\psi]^2 \rangle_{\gamma_l} + \frac{1}{2} \langle |U \cdot n|, (\psi^-)^2 \rangle_{\Gamma_I} + \frac{1}{2} \langle U \cdot n, (\psi^-)^2 \rangle_{\Gamma_O} \\ &\quad + \frac{1}{2} \sum_e (\nabla \cdot U, \psi^2)_{\Omega_e} \\ &= \frac{1}{2} \sum_l \langle |U \cdot n_l|, [\psi]^2 \rangle_{\gamma_l} + \frac{1}{2} \langle |U \cdot n|, (\psi^-)^2 \rangle_{\Gamma} + \frac{1}{2} \sum_e (\nabla \cdot U, \psi^2)_{\Omega_e}. \end{aligned}$$

Substituting (33) into (31), we obtain

$$\begin{aligned} (34) \quad & \sum_e (\psi_t, \psi)_{\Omega_e} + \frac{1}{2} \sum_l \langle |U \cdot n_l|, [\psi]^2 \rangle_{\gamma_l} + \frac{1}{2} \langle |U \cdot n|, (\psi^-)^2 \rangle_{\Gamma} \\ &= \sum_e \left[ (\theta_t, \psi)_{\Omega_e} + ((U - u) \Pi c, \nabla \psi)_{\Omega_e} - (u \theta, \nabla \psi)_{\Omega_e} + \frac{1}{2} (\nabla \cdot U, \psi^2)_{\Omega_e} \right. \\ &\quad \left. + (\Pi c \nabla \cdot U, \psi)_{\Omega_e} \right] \\ &\quad - \sum_l [\langle U \cdot n_l (c - \Pi c^u), [\psi] \rangle_{\gamma_l} - \langle (u - U) \cdot n_l c, [\psi] \rangle_{\gamma_l}] \\ &\quad + \langle U \cdot n (c - \Pi c^-), \psi^- \rangle_{\Gamma_O} + \langle (u - U) \cdot n c, \psi^- \rangle_{\Gamma_O}. \\ &\equiv \mathcal{T}_1 + \dots \mathcal{T}_9. \end{aligned}$$

We now analyze the terms  $\mathcal{T}_1$  through  $\mathcal{T}_9$ .

In the arguments below, let  $t^* \in [0, T]$  denote the time at which  $\|\psi(\cdot, t)\|$  is maximized. Let  $K$  denote a generic positive constant, and  $\epsilon$  a generic small positive constant. We will also use the standard inequality,

$$ab \leq \frac{K}{2} a^2 + \frac{1}{2K} b^2, \quad a, b \in \mathbb{R}, K > 0.$$

First, by the definition of  $\Pi c$ ,

$$(35) \quad \mathcal{T}_1 = \sum_e (\theta_t, \psi)_{\Omega_e} = 0.$$

Next,

$$\begin{aligned} \mathcal{T}_2 &= \sum_e ((U - u)\Pi c, \nabla \psi)_{\Omega_e} \\ &= \sum_e ((U - u)(c - \theta), \nabla \psi)_{\Omega_e} \\ &\leq \sum_e [ \|U - u\|_{\Omega_e} (\|c\|_{\infty} + \|\theta\|_{\infty}) \|\nabla \psi\|_{\Omega_e} ]. \end{aligned}$$

For  $c$  smooth,

$$\|c\|_{\infty} + \|\theta\|_{\infty} \leq K.$$

By standard inverse estimates for polynomials,

$$(36) \quad \|\nabla \psi\|_{\Omega_e} \leq K h_e^{-1} \|\psi\|_{\Omega_e},$$

Thus,

$$\mathcal{T}_2 \leq K \sum_e h_e^{-1} \|U - u\|_{\Omega_e} \|\psi\|_{\Omega_e}.$$

Integrating in time,

$$(37) \quad \int_0^{t^*} \mathcal{T}_2 dt \leq \epsilon \|\psi(\cdot, t^*)\|^2 + K (t^*)^2 \sum_e h_e^{-2} \|U - u\|_{\Omega_e}^2.$$

For the next term, let  $\Pi_0 u$  denote the projection of each component of  $u$  into piecewise constants,

$$(u - \Pi_0 u, 1)_{\Omega_e} = 0.$$

Thus,

$$\|u - \Pi_0 u\|_{\infty, \Omega_e} \leq K \|u\|_{W_{\infty}^1} h_e.$$

Then, by the definition of  $\Pi c$ , and (36),

$$\begin{aligned} \mathcal{T}_3 &= \sum_e (u\theta, \nabla \psi)_{\Omega_e} \\ &= \sum_e ((u - \Pi_0 u)\theta, \nabla \psi)_{\Omega_e} \\ &\leq K \sum_e h_e \|\theta\|_{\Omega_e} \|\nabla \psi\|_{\Omega_e} \\ &\leq K \sum_e \|\theta\|_{\Omega_e} \|\psi\|_{\Omega_e}. \end{aligned}$$

Integrating in time,

$$(38) \quad \int_0^{t^*} \mathcal{T}_3 dt \leq \epsilon \|\psi(\cdot, t^*)\|^2 + K \left( \int_0^{t^*} \|\theta(\cdot, t)\| dt \right)^2.$$

Continuing,

$$\begin{aligned} \mathcal{T}_4 &= \frac{1}{2} \sum_e (\nabla \cdot U, \psi^2)_{\Omega_e} \\ &\leq \frac{1}{2} \|\nabla \cdot U\|_{\infty} \|\psi\|^2. \end{aligned}$$

Thus, by assumption **A2**, for  $h$  sufficiently small

$$(39) \quad \begin{aligned} \int_0^{t^*} \mathcal{T}_4 dt &\leq \frac{1}{2} \|\nabla \cdot U\|_{\infty} \int_0^{t^*} \|\psi\|^2 dt \\ &\leq \frac{t^*}{2} \|\nabla \cdot U\|_{\infty} \|\psi(\cdot, t^*)\|^2 \\ &\leq \frac{1}{4} \|\psi(\cdot, t^*)\|^2. \end{aligned}$$

Similarly,

$$(40) \quad \begin{aligned} \int_0^{t^*} \mathcal{T}_5 dt &= \int_0^{t^*} \sum_e (\Pi c \nabla \cdot U, \psi)_{\Omega_e} \\ &= \int_0^{t^*} \sum_e ((c - \theta) \nabla \cdot U, \psi)_{\Omega_e} \\ &\leq \int_0^{t^*} (\|c\|_{\infty} + \|\theta\|_{\infty}) \sum_e \|\nabla \cdot U\|_{\Omega_e} \|\psi\|_{\Omega_e} \\ &\leq K(t^*)^2 \sum_e \|\nabla \cdot U\|_{\Omega_e}^2 + \epsilon \|\psi(\cdot, t^*)\|^2. \end{aligned}$$

Next,

$$(41) \quad \begin{aligned} \mathcal{T}_6 &= - \sum_l \langle U \cdot n_l (c - \Pi c^u), [\psi] \rangle_{\gamma_l} \\ &\leq K \sum_l \| |U \cdot n_l|^{1/2} (c - \Pi c^u) \|_{\gamma_l}^2 + \frac{1}{4} \sum_l \| |U \cdot n_l|^{1/2} [\psi] \|_{\gamma_l}^2. \end{aligned}$$

For the next term, we need the following result, which can be found in [3]. Assuming  $\Omega_e$  has a Lipschitz boundary,

$$(42) \quad \|\psi\|_{\partial \Omega_e}^2 \leq \|\psi\|_{\Omega_e} \|\psi\|_{H^1(\Omega_e)}.$$

Consider

$$\begin{aligned} \mathcal{T}_7 &= \sum_l \langle (u - U) \cdot n_l c, [\psi] \rangle_{\gamma_l} \\ &\leq K \sum_l \| (u - U) \cdot n_l \|_{\gamma_l} \| [\psi] \|_{\gamma_l} \end{aligned}$$

$$\begin{aligned}
&\leq K \sum_l \|(u - U) \cdot n_l\|_{\gamma_l} \left( \sum_{e: \partial\Omega_e \cap \gamma_l \neq \emptyset} \|\psi\|_{\Omega_e}^{1/2} \|\psi\|_{H^1(\Omega_e)}^{1/2} \right) \\
&\leq K \sum_l \|(u - U) \cdot n_l\|_{\gamma_l} \left( \sum_{e: \partial\Omega_e \cap \gamma_l \neq \emptyset} h_e^{-1/2} \|\psi\|_{\Omega_e} \right) \\
&\leq K \sum_l h_l^{-1/2} \|(u - U) \cdot n_l\|_{\gamma_l} \left( \sum_{e: \partial\Omega_e \cap \gamma_l \neq \emptyset} \|\psi\|_{\Omega_e} \right),
\end{aligned}$$

where

$$h_l = \min_{e: \partial\Omega_e \cap \gamma_l \neq \emptyset} h_e.$$

Integrating in time, we find

$$(43) \quad \int_0^{t^*} \mathcal{T}_7 dt \leq K(t^*)^2 \sum_l h_l^{-1} \|(u - U) \cdot n_l\|_{\gamma_l}^2 + \epsilon \|\psi(\cdot, t^*)\|^2.$$

Similar to  $\mathcal{T}_6$ ,

$$(44) \quad \begin{aligned} \mathcal{T}_8 &= \langle U \cdot n(c - \Pi c^-), \psi^- \rangle_{\Gamma_O} \\ &\leq K \|U \cdot n\|_{\Gamma_O}^2 \|c - \Pi c^-\|_{\Gamma_O}^2 + \frac{1}{4} \|U \cdot n\|_{\Gamma_O}^2 \|\psi^-\|_{\Gamma_O}^2. \end{aligned}$$

Similar to  $\mathcal{T}_7$ ,

$$\begin{aligned}
\mathcal{T}_9 &= \langle c(u - U) \cdot n, \psi^- \rangle_{\Gamma_O} \\
&= \sum_{e: \partial\Omega_e \cap \Gamma_O \neq \emptyset} \langle c(u - U) \cdot n, \psi^- \rangle_{\partial\Omega_e \cap \Gamma_O} \\
&\leq K \sum_{e: \partial\Omega_e \cap \Gamma_O \neq \emptyset} \|(u - U) \cdot n\|_{\partial\Omega_e \cap \Gamma_O} \|\psi^-\|_{\partial\Omega_e \cap \Gamma_O} \\
&\leq K \sum_{e: \partial\Omega_e \cap \Gamma_O \neq \emptyset} h_e^{-1/2} \|(u - U) \cdot n\|_{\partial\Omega_e \cap \Gamma_O} \|\psi\|_{\Omega_e}.
\end{aligned}$$

Thus

$$(45) \quad \int_0^{t^*} \mathcal{T}_9 dt \leq K(t^*)^2 \sum_{e: \partial\Omega_e \cap \Gamma_O \neq \emptyset} h_e^{-1} \|(u - U) \cdot n\|_{\partial\Omega_e \cap \Gamma_O}^2 + \epsilon \|\psi(\cdot, t^*)\|^2.$$

Integrating (34) in time, inserting the bounds (35)-(45), choosing  $\epsilon$  sufficiently small, we find

$$\begin{aligned}
(46) \quad \|\psi(\cdot, t^*)\|^2 &\leq K(t^*)^2 \sum_e [h_e^{-2} \|U - u\|_{\Omega_e}^2 + \|\nabla \cdot U\|_{\Omega_e}^2] \\
&\quad + K(t^*)^2 \sum_l h_l^{-1} \|(u - U) \cdot n_l\|_{\gamma_l}^2 \\
&\quad + K(t^*)^2 \sum_{e: \partial\Omega_e \cap \Gamma_O \neq \emptyset} h_e^{-1} \|(u - U) \cdot n\|_{\partial\Omega_e \cap \Gamma_O}^2
\end{aligned}$$

$$\begin{aligned}
& +K \int_0^{t^*} \left[ \sum_l \| |U \cdot n_l|^{1/2} (c - \Pi c^u) \|_{\gamma_l}^2 + \| |U \cdot n|^{1/2} (c - \Pi c^-) \|_{\Gamma_o}^2 \right] dt \\
& +K \left( \int_0^{t^*} \|\theta(\cdot, t)\| dt \right)^2.
\end{aligned}$$

Let

$$k = \min_e k_e,$$

then for  $c$  sufficiently smooth, the last three terms on the right side of (46) are  $\mathcal{O}(h^{2k+1})$ . Therefore, we have the following result:

**THEOREM 3.1.** *If assumptions **A1** and **A2** hold on the approximate velocity  $U$ , and  $c$  and  $u$  are sufficiently smooth, then*

$$\begin{aligned}
\max_{[0, T]} \|\psi(\cdot, t)\|^2 & \leq KT^2 \sum_e [h_e^{-2} \|U - u\|_{\Omega_e}^2 + \|\nabla \cdot U\|_{\Omega_e}^2] \\
& +KT^2 \sum_l h_l^{-1} \|(u - U) \cdot n_l\|_{\gamma_l}^2 \\
& +KT^2 \sum_{e: \partial\Omega_e \cap \Gamma_o \neq \emptyset} h_e^{-1} \|(u - U) \cdot n\|_{\partial\Omega_e \cap \Gamma_o}^2 + Kh^{2k+1}.
\end{aligned}$$

**4. A two-dimensional example.** In this section, we consider the application of the method above to the problem,

$$c_t + \nabla \cdot (uc) = fc, \quad (x, t) \in \Omega \times (0, T],$$

where  $\Omega = [0, 1] \times [0, 1]$  and  $f$  is a smooth source term. We assume the velocity  $u = (u^x, u^y)$  satisfies

$$(47) \quad \nabla \cdot u = f.$$

We also assume there exists a potential  $p$  such that

$$(48) \quad u = -K\nabla p,$$

which is the well-known Darcy's Law in porous media flow, where  $K$  is the hydraulic conductivity of the porous medium, or the ratio of the permeability of the medium to the fluid viscosity.

Choosing a time step  $\Delta t$ , discretizing  $\Omega$  into uniform grid blocks

$$B_{ij} = [x_{i-1/2}, x_{i+1/2}] \times [y_{j-1/2}, y_{j+1/2}]$$

of size  $h^2$ , and approximating  $c(\cdot, t^k)$  on  $B_{ij}$  by a constant  $C_{ij}^k$ , we obtain the upwind scheme

$$\begin{aligned}
(49) \quad & \frac{C_{ij}^{k+1} - C_{ij}^k}{\Delta t} + \frac{u_{i+1/2, j}^x (C_{i+1/2, j}^k)^u - u_{i-1/2, j}^x (C_{i-1/2, j}^k)^u}{h} \\
& + \frac{u_{i, j+1/2}^y (C_{i, j+1/2}^k)^u - u_{i, j-1/2}^y (C_{i, j-1/2}^k)^u}{h} = f_{ij} C_{ij}^{k+1}.
\end{aligned}$$

Here  $(C_{i+1/2,j}^k)^u$  is the upwind value of  $C^k$  at  $(x_{i+1/2}, y_j)$ ,  $u_{i+1/2,j}^x$  is the average value of  $u^x$  over the edge  $x = x_{i+1/2}$ ,  $y_{j-1/2} \leq y \leq y_{j+1/2}$ , and  $f_{ij}$  is the average value of  $f$  over  $B_{ij}$ , so that from (47),

$$(50) \quad hf_{ij} = u_{i+1/2,j}^x - u_{i-1/2,j}^x + u_{i,j+1/2}^y - u_{i,j-1/2}^y.$$

We now demonstrate that the method (49) satisfies a maximum principle. Let

$$a^\pm = \text{sign}(u_{i\pm 1/2,j}^x),$$

and

$$b^\pm = \text{sign}(u_{i,j\pm 1/2}^y).$$

Then (49) can be rewritten as

$$\begin{aligned} C_{ij}^{k+1}(1 - \Delta t f_{ij}) = C_{ij}^k - \frac{\Delta t}{h} & \left[ u_{i+1/2,j}^x \left\{ \frac{a^+ + 1}{2} C_{ij}^k - \frac{a^+ - 1}{2} C_{i+1,j}^k \right\} \right. \\ & - u_{i-1/2,j}^x \left\{ \frac{a^- + 1}{2} C_{i-1,j}^k - \frac{a^- - 1}{2} C_{i,j}^k \right\} \\ & + u_{i,j+1/2}^y \left\{ \frac{b^+ + 1}{2} C_{ij}^k - \frac{b^+ - 1}{2} C_{i,j+1}^k \right\} \\ & \left. - u_{i,j-1/2}^y \left\{ \frac{b^- + 1}{2} C_{i,j-1}^k - \frac{b^- - 1}{2} C_{ij}^k \right\} \right], \end{aligned}$$

or

$$(51) \quad C_{ij}^{k+1}(1 - \Delta t f_{ij}) = \alpha C_{ij}^k + \beta C_{i+1,j}^k + \rho C_{i-1,j}^k + \sigma C_{i,j+1}^k + \kappa C_{i,j-1}^k,$$

where

$$(52) \quad \alpha = 1 - \frac{\Delta t}{h} \left[ u_{i+1/2,j}^x \frac{a^+ + 1}{2} + u_{i-1/2,j}^x \frac{a^- - 1}{2} \right. \\ \left. + u_{i,j+1/2}^y \frac{b^+ + 1}{2} + u_{i,j-1/2}^y \frac{b^- - 1}{2} \right],$$

$$(53) \quad \beta = \frac{\Delta t}{h} u_{i+1/2,j}^x \frac{a^+ - 1}{2},$$

$$(54) \quad \rho = \frac{\Delta t}{h} u_{i-1/2,j}^x \frac{a^- + 1}{2},$$

$$(55) \quad \sigma = \frac{\Delta t}{h} u_{i,j+1/2}^y \frac{b^+ - 1}{2},$$

$$(56) \quad \kappa = \frac{\Delta t}{h} u_{i,j-1/2}^y \frac{b^- + 1}{2}.$$

For  $\Delta t$  satisfying the CFL constraint

$$(57) \quad \frac{2\Delta t}{h} (\|u^x\|_\infty + \|u^y\|_\infty) < 1,$$

we find that  $\alpha > 0$ . By definition,  $\beta$ ,  $\rho$ ,  $\sigma$  and  $\kappa$  are nonnegative. Therefore,

$$\begin{aligned} 0 & < \alpha + \beta + \rho + \sigma + \kappa \\ & = 1 - \frac{\Delta t}{h} \left[ u_{i+1/2,j}^x - u_{i-1/2,j}^x + u_{i,j+1/2}^y - u_{i,j-1/2}^y \right] \\ (58) \quad & = 1 - \Delta t f_{ij}, \end{aligned}$$

by (50). Let

$$C_{\max}^k = \max_{i,j} |C_{ij}^k|.$$

Then, by (51) and (58),

$$\begin{aligned} |C_{ij}^{k+1}|(1 - \Delta t f_{ij}) &\leq (\alpha + \beta + \rho + \sigma + \kappa) C_{\max}^k, \\ &= (1 - \Delta t f_{ij}) C_{\max}^k. \end{aligned}$$

Hence, we have the stability bound

$$(59) \quad |C_{ij}^{k+1}| \leq C_{\max}^k.$$

Now, suppose we approximate  $u$  by  $U$ , then the maximum principle argument above carries through with  $U$  replacing  $u$  up to the conclusion (59). In order for (59) to hold, we need

$$(60) \quad hf_{ij} = U_{i+1/2,j}^x - U_{i-1/2,j}^x + U_{i,j+1/2}^y - U_{i,j-1/2}^y \equiv (\nabla \cdot U)_{ij}.$$

Suppose (60) is only satisfied approximately, then we modify the scheme (49) by adding the correction term  $C_{ij}^{k+1}(\nabla \cdot U_{ij} - f_{ij})$  to the right hand side, obtaining

$$(61) \quad \begin{aligned} &\frac{C_{ij}^{k+1} - C_{ij}^k}{\Delta t} + \frac{U_{i+1/2,j}^x (C_{i+1/2,j}^k)^u - U_{i-1/2,j}^x (C_{i-1/2,j}^k)^u}{h} \\ &+ \frac{U_{i,j+1/2}^y (C_{i,j+1/2}^k)^u - U_{i,j-1/2}^y (C_{i,j-1/2}^k)^u}{h} = (\nabla \cdot U)_{ij} C_{ij}^{k+1}. \end{aligned}$$

That is, the corrected method amounts to replacing  $f_{ij}$  on the right side of (49) by  $(\nabla \cdot U)_{ij}$ . Thus, we find for the corrected method

$$(62) \quad C_{ij}^{k+1}(1 - \Delta t(\nabla \cdot U)_{ij}) = \alpha C_{ij}^k + \beta C_{i+1,j}^k + \rho C_{i-1,j}^k + \sigma C_{i,j+1}^k + \kappa C_{i,j-1}^k,$$

where  $\alpha, \beta$ , etc., have the same definitions as before with  $u$  replaced by  $U$ . Following the argument that led to (59), we find that the corrected method (61) satisfies the same stability bound, assuming  $\Delta t$  satisfies the CFL constraint

$$\frac{2\Delta t}{h} (\|U^x\|_\infty + \|U^y\|_\infty) < 1.$$

We conclude with a numerical example. We assume (47) with the source function

$$(63) \quad f(x, y) = e^{-100(x-.05)^2(y-.05)^2} - e^{-100(x-.95)^2(y-.95)^2}.$$

We take as the initial condition a step function

$$(64) \quad c^0(x, y) = \begin{cases} 1, & 0 \leq x \leq .1, 0 \leq y \leq .1, \\ 0, & \text{otherwise.} \end{cases}$$

We assume  $K = 1$  in (48), and assume the boundary condition

$$(65) \quad u \cdot n = 0,$$

on  $\partial\Omega$ . We approximate the velocity two different ways. In one case we apply the mixed finite element method with lowest order Raviart-Thomas approximating spaces [18] to the system (47)-(48). Using certain integration rules, this method reduces to a cell-centered finite difference scheme for the potential  $p$  [21],

$$(66) \quad -\frac{P_{i+1,j} - 2P_{ij} + P_{i-1,j}}{h^2} - \frac{P_{i,j+1} - 2P_{ij} + P_{i,j-1}}{h^2} = f_{ij},$$

where  $P_{ij} \approx p(x_i, y_j)$  and  $(x_i, y_j)$  is the midpoint of  $B_{ij}$ . The no-flow condition (65) is enforced through the difference scheme as follows. For  $i = 1$ , for example, we modify (66) to be

$$-\frac{P_{2j} - P_{1j}}{h^2} - \frac{P_{1,j+1} - 2P_{1j} + P_{1,j-1}}{h^2} = f_{1j}.$$

The numerical velocity  $U = (U^x, U^y)$  for the mixed finite element is computed by

$$(67) \quad U_{i+1/2,j}^x = -\frac{P_{i+1,j} - P_{ij}}{h},$$

with a similar definition for  $U_{i,j+1/2}^y$ , and the no-flow condition is enforced by setting, for example,  $U_{1/2,j}^x = 0$ . By (66) and (67),  $U$  satisfies (60) over each element.

In the second case, we note that (47) and (48) imply that

$$(68) \quad -\Delta p = f,$$

and approximate  $p$  by a point-centered finite difference scheme:

$$(69) \quad -\frac{P_{i+3/2,j+1/2} - 2P_{i+1/2,j+1/2} + P_{i-1/2,j+1/2}}{h^2} - \frac{P_{i+1/2,j+3/2} - 2P_{i+1/2,j+1/2} + P_{i+1/2,j-1/2}}{h^2} = f_{i+1/2,j+1/2},$$

where  $P_{i+1/2,j+1/2} \approx p(x_{i+1/2}, y_{j+1/2})$ . The scheme (69) is modified similarly to (66) to weakly enforce the no-flow boundary condition. This point-centered scheme can be derived from the standard piecewise linear Galerkin finite element method applied to (68), on a mesh obtained by dividing each block  $B_{ij}$  into two right triangles, with all diagonals oriented from lower left corner to upper right corner (or vice versa). We approximate the velocity ( $u_{i+1/2,j}^x$ , for example) similar to (67) by setting

$$(70) \quad U_{i+1/2,j}^x = -\frac{\bar{P}_{i+1,j} - \bar{P}_{i,j}}{h},$$

where

$$\bar{P}_{i,j} = (P_{i+1/2,j+1/2} + P_{i-1/2,j+1/2} + P_{i+1/2,j-1/2} + P_{i-1/2,j-1/2})/4.$$

We again enforce (65) directly, by setting, for example  $U_{1/2,j}^x = 0$ . The equation (70) is only one of several post-processing techniques that one could use to calculate the numerical velocity; this particular approximation does not satisfy (60).

In Figure 8a, the approximate solution  $C$  from the method (61), obtained on a  $40 \times 40$  uniform grid at time  $T = 10$  (about 20 times steps), with the mixed finite element velocity approximation (67), is contoured. The contour levels, from right

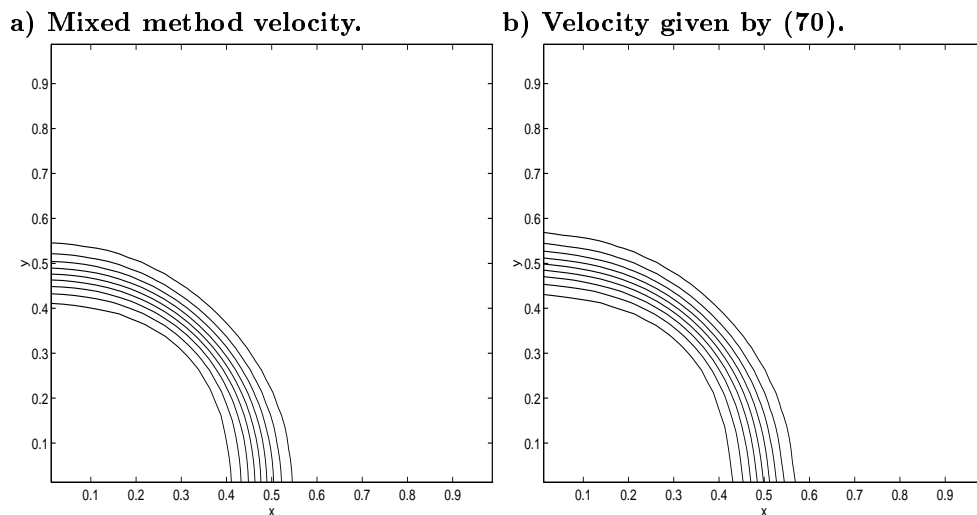


FIG. 8. Comparison of solutions at time  $T = 10$  on  $40 \times 40$  uniform grid.

to left, range from .1 to .9 in increments of .1. In Figure 8b, the solution obtained from the same method, using the velocity approximation (70) is plotted. We see good agreement between the two solutions, with the solution front in Figure 8b slightly more advanced than that of Figure 8a, indicating that the solution in Figure 8b has slightly more mass. In fact, the total mass for this solution is .199, while the solution in Figure 8a has mass .184. Total mass is computed as

$$\text{total mass at time } t = \int_{\Omega} C(x, t) dx.$$

The solutions for the two cases on an  $80 \times 80$  uniform grid at the same time are given in Figures 9a and 9b. These solutions have better resolution than those given in the previous figures. The two solutions at later time,  $T = 30$ , are given in Figures 10a and 10b. The total mass for the solution in Figure 9b is .1925, while the total mass in Figure 9a is again .184, thus the difference in the masses has decreased from the  $40 \times 40$  case. The masses for the solutions in Figures 10a and 10b are .547 and .577, respectively.

Since the source function  $f$  is smooth, we expect that the pressure  $P$  generated by (69) is second order accurate, and the velocity  $U$  perhaps only first order accurate. However, the error in  $\nabla \cdot U$  for this case also seems to be approaching zero as the mesh is refined. For  $10 \times 10$ ,  $20 \times 20$ ,  $40 \times 40$  and  $80 \times 80$  uniform grids, the error  $\|f - \nabla \cdot U\|_{\infty}$  was found to be  $1.09 \times 10^{-3}$ ,  $4.99 \times 10^{-4}$ ,  $1.75 \times 10^{-4}$  and  $4.64 \times 10^{-5}$ .

Finally, we remark that the method (49), with the nonconservative velocity approximation (70), gives a significantly different solution than the ones in Figures 9a and 9b, as shown in Figure 11. Therefore, simply adding the correction term to (49) seems to give a much more physically realistic solution.

#### REFERENCES

- [1] T. ARBOGAST, S. BRYANT, C. DAWSON, F. SAAF, AND C. WANG, *Computational methods for multiphase flow and reactive transport problems arising in subsurface contaminant remediation*, J. Comp. Appl. Math., 74 (1996), pp. 19–32.

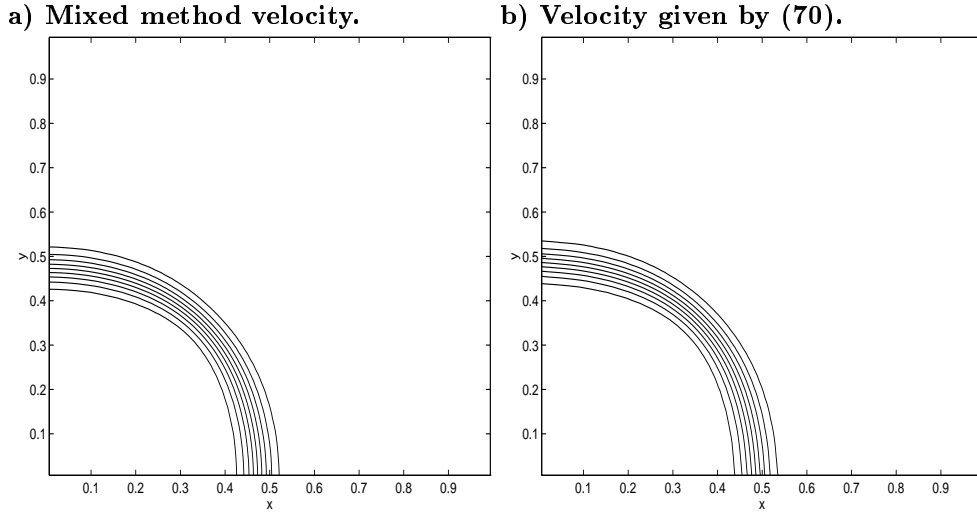


FIG. 9. Comparison of solutions at time  $T = 10$  on  $80 \times 80$  uniform grid.

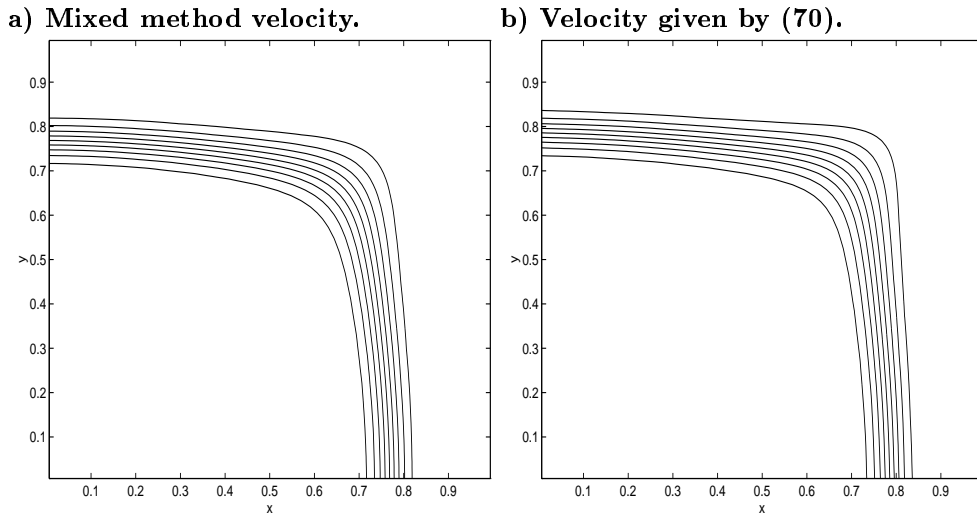


FIG. 10. Comparison of solutions at time  $T = 30$  on  $80 \times 80$  uniform grid.

- [2] R. BERGER, W. MARTIN, R. MCADORY, AND J. SCHMIDT, *Galveston bay 3d model study, channel deepening, circulation, and salinity results*, in Proceedings of the 3rd International Conference on Estuarine and Coastal Modeling, Sept. 8-10, Oak Brook, IL, 1993, pp. 1–13.
- [3] S. BRENNER AND L. R. SCOTT, *The Mathematical Theory of Finite Element Methods*, Springer Verlag, New York, 1994.
- [4] Q. CHEN, D. ZHAO, I. G. Q. TABIOS, AND H. W. SHEN, *2D coupled water quality model for industrial effluent transport*, in Proceedings of the 1998 International Water Resource Engineering Conference, vol. 2, ASCE, 1998, pp. 1637–1642.
- [5] S. CHIPPADA, C. DAWSON, M. MARTINEZ, AND M. F. WHEELER, *A projection method for constructing a mass conservative velocity field*, *Comput. Meth. Appl. Mech. Engrg.*, 151 (1998), pp. 105–129.
- [6] B. COCKBURN, S. HOU, AND C. W. SHU, *TVB Runge-Kutta local projection discontinuous galerkin finite element method for conservations laws IV: The multidimensional case*, *Math. Comp.*, 54 (1990), pp. 545–581.

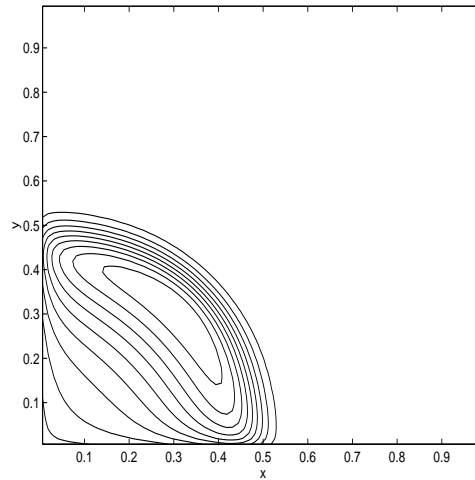


FIG. 11. Scheme (49) with nonconservative velocity (70) at  $T = 10$  on  $80 \times 80$  uniform grid.

- [7] B. COCKBURN, S. Y. LIN, AND C. W. SHU, *TVB Runge-Kutta local projection discontinuous Galerkin finite element method for conservations laws III: One dimensional systems*, J. Comput. Phys., 84 (1989), pp. 90–113.
- [8] B. COCKBURN AND C. W. SHU, *TVB Runge-Kutta local projection discontinuous Galerkin finite element method for scalar conservations laws II: General framework*, Math. Comp., 52 (1989), pp. 411–435.
- [9] ———, *The Runge-Kutta local projection  $P^1$ -discontinuous Galerkin method for scalar conservations laws*,  $M^2AN$ , 25 (1991), pp. 337–361.
- [10] ———, *TVB Runge-Kutta discontinuous Galerkin finite element method for conservations laws V: Multidimensional systems*, J. Comput. Physics, 141 (1998), pp. 199–224.
- [11] C. DAWSON AND V. AIZINGER, *Upwind mixed methods for transport equations*. Computational Geosciences, to appear.
- [12] H.-J. G. DIERSCH, *Shock-capturing finite-element technique for unsaturated-saturated flow and transport problems*, in Proceedings of the 12th International Conference on Computational Methods in Water Resources, vol. 1, Computational Mechanics Publications, 1998, pp. 207–214.
- [13] M. S. DORTH, C. RUIZ, T. GERAL, AND R. W. HALL, *Three-dimensional contaminant transport/fate model*, in Proceedings of the 5th International Conference on Estuarine and Coastal Modeling, ASCE, 1997, pp. 75–89.
- [14] C. GALLO AND G. MANZINI, *2-D numerical modeling of bioremediation in heterogeneous saturated soils*, Transport in Porous Media, 31 (1998), pp. 67–88.
- [15] ———, *Mixed finite element/volume approach for solving biodegradation transport in groundwater*, Int. J. Numer. Meth. Fluids, 26 (1998), pp. 533–556.
- [16] R. J. LEVEQUE, *Numerical Methods for Conservation Laws*, Birkhauser, Basel, 1992.
- [17] J. R. A. LUETTICH, J. J. WESTERINK, AND N. W. SCHEFFNER, *Adcirc: An advanced three-dimensional circulation model for shelves, coasts and estuaries*, tech. rep., Department of the Army, U.S. Army Corps of Engineers, Washington, DC, 20314-1000, December 1991.
- [18] P. A. RAVIART AND J. M. THOMAS, *A mixed finite element method for second order elliptic problems*, in Mathematical Aspects of Finite Element Methods: Lecture Notes in Mathematics, I. Galligani and E. Magenes, eds., vol. 606, Springer-Verlag, Berlin, 1977, pp. 292–315.
- [19] S. SANKARANARAYANAN, N. J. SHANKAR, AND H. F. CHEONG, *Three-dimensional finite difference model for transport of conservative pollutants*, Ocean Engineering, 25 (1998), pp. 425–442.
- [20] P. SIEGEL, R. MOSE, P. ACKERER, AND J. JAFFRE, *Solution of the advection-diffusion equation using a combination of discontinuous and mixed finite elements*, Int. J. Numer. Meth. Fluids, 24 (1997), pp. 595–613.
- [21] A. WEISER AND M. F. WHEELER, *On convergence of block-centered finite differences for elliptic problems*, SIAM J. Numer. Anal., 25 (1988), pp. 351–375.

- [22] D. ZHAO, J. S. LAI, AND W. S. HSIEH, *Two-dimensional contaminant transport model with high resolution upwind scheme*, in Proceedings of the 1994 ASCE National Conference on Hydraulic Engineering, ASCE, 1994, pp. 135–139.